Peer-reviewed version available at J. Imaging 2018, 4, 3; doi:10.3390/jimaging4010003

Article

Texture Based Quality Analysis of Simulated Synthetic Ultrasound Images Using Local Binary Patterns

Prerna Singh [1,*], Ramakrishnan Mukundan [1] and Rex De Ryke[2]

[1] Department of Computer Science and Software Engineering, University of Canterbury; New Zealand. prerna.singh@pg.canterbury.ac.nz, mukundan@canterbury.ac.nz
[2] Radiology Services, Christchurch District Health Board, New Zealand; Rex.DeRyke@cdhb.health.nz
* Correspondence: prerna.singh@pg.canterbury.ac.nz; Tel.: +64-2041175855

Abstract: Speckle noise reduction is an important area of research in the field of ultrasound image processing. Several algorithms for speckle noise characterization and analysis have been recently proposed in the area. Synthetic ultrasound images can play a key role in noise evaluation methods as they can be used to generate a variety of speckle noise models under different interpolation and sampling schemes, and can also provide valuable ground truth data for estimating the accuracy of the chosen methods. However, not much work has been done in the area of modelling synthetic ultrasound images, and in simulating speckle noise generation to get images that are as close as possible to real ultrasound images. An important aspect of simulated synthetic ultrasound images is the requirement for extensive quality assessment for ensuring that they have the texture characteristics and gray-tone features of real images. This paper presents texture feature analysis of synthetic ultrasound images using local binary patterns (LBP) and demonstrates the usefulness of a set of LBP features for image quality assessment. Experimental results presented in the paper clearly show how these features could provide an accurate quality metric that correlates very well with subjective evaluations performed by clinical experts.

Keywords: ultrasound image analysis; speckle noise; synthetic ultrasound images; texture features; local binary patterns; image quality assessment

1. Introduction

Ultrasound images are known to have poor signal-to-noise ratio, yet they are low cost non-invasive techniques in diagnostic radiology and hence extensively used in clinical applications. Several new ultrasound image analysis algorithms are currently being researched for noise reduction [1-3], segmentation [4], registration and volume reconstruction [5]. Online ultrasound image databases are now becoming increasingly available and this has greatly benefitted researchers in obtaining reference images for testing and evaluating algorithms [5-7].

The speckle noise in ultrasound images degrades the fine details and edge definitions, and limits the contrast resolution by making it difficult to detect small and low contrast lesions in the body. Therefore, algorithms for ultrasound image filtering and analysis primarily focus on the characteristics of speckle noise and try to minimize its effects on image interpretation [8]. To analyse the effectiveness or accuracy of speckle reduction techniques, it is necessary to add controlled noise to ideal noiseless images [2]. In the absence of such noiseless ground truth images, researchers commonly use standard non-ultrasound test images (eg. Lena, Mandrill etc.) or discrete gray-level patterns and model speckle noise on those images to perform algorithm evaluation. This paper addresses the need for generating accurate synthetic models of ultrasound image formation for applications in speckle noise analysis. A synthetic ultrasound image can be sampled using a configuration of points that correspond to either linear or sector scan modes of ultrasound imaging, and interpolated later after generating speckle noise at the sampled points to obtain visually realistic

effects. Synthetic images can therefore be used to generate simulated ultrasound images with a wide range of image and noise characteristics useful for filtering methods and noise analysis.

Statistical and empirical methods of generating speckle lack realism since several important characteristics of the image acquisition models are often ignored. There are only very limited algorithms reported in literature for speckle simulation based on image acquisition modeling. Perreault and Auclair-Fortier [9] proposed an efficient simulation model of ultrasound images based on a radial-polar configuration of sampling points and a speckle noise simulation algorithm. We extend their work by considering different types of sampling and interpolation schemes and by performing detailed experimental analysis to compare their effectiveness in producing realistic speckle simulation. Their work used images of Lena and Barbara for generating the simulated images with speckle noise. However, for generating highly realistic synthetic models, we require images that have texture features and intensity characteristics that closely match the features of real ultrasound images. Therefore, a very important aspect of synthetic image modelling algorithms is quality assessment. In the proposed method, the base synthetic image is modified as outlined above using the acquisition model, speckle noise simulation and interpolation of the sampled points. Second order texture feature analysis using Gray level co-occurrence matrix (GLCM) has been already performed in our recently proposed work [12], where we felt the need for more robust texture descriptors that would show consistent behavior with variation of image quality induced by changes in the modeling parameters. This paper addresses this problem by considering local binary patterns (LBP) for representing the texture content in the images. To the authors' knowledge, no prior work has been reported on image texture feature based quality assessment of realistic synthetic ultrasound images using local binary patterns. In this paper, the quality of the generated synthetic image texture features are analysed using LBP [10, 11], and correlated with subjective evaluation scores assigned by clinicians.

The paper presents the complete framework for the development of synthetic ultrasound images including the set of processes in both simulation and evaluation stages. It also presents the results of an exhaustive experimental analysis of texture features using LBP for each of the three sampling methods. The presented results clearly show the usefulness of LBP in accurately characterizing the texture features and therefore the overall quality of modelled synthetic images. This paper is organized as follows: The next section gives a brief outline of the images used and the methods in the processing pipeline. Section 3 describes the simulation model in detail. Section 4 presents the synthetic ultrasound images with variations of modeling parameters. Section 5 gives an overview of local binary patterns. Section 6 presents experimental results and their evaluations using LBP. Section 7 gives a summary of the work presented in the paper and outlines future directions.

2. Materials and Methods

For experimental work presented in the paper, the reference images of real ultrasound images were sourced from the online ultrasound image gallery [7]. These are ultrasound scans of the liver, and have very similar image features, intensity distribution and noise content. Figure 1 shows three such reference images and their histogram to show intensity distribution of each image.

Preprints (www.preprints.org) | NOT PEER-REVIEWED | Posted: 30 October 2017 doi:10.20944/preprints201710.0181.v1

Peer-reviewed version available at J. Imaging 2018, 4, 3; doi:10.3390/jimaging4010003

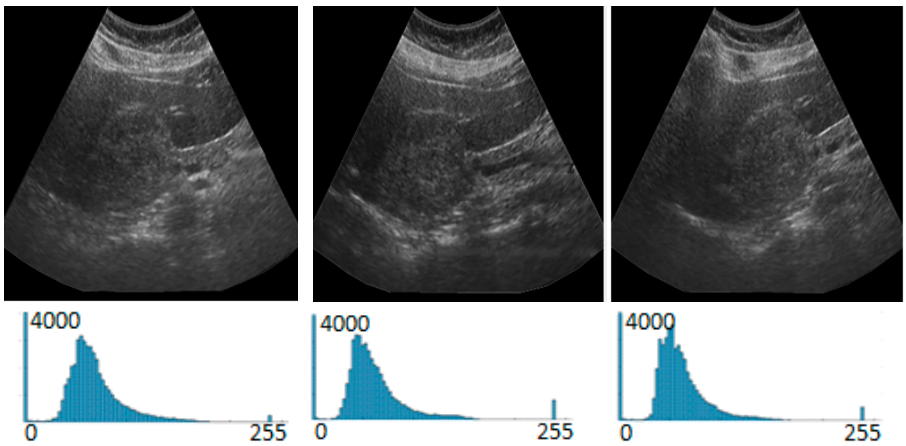

Figure 1. Reference ultrasound images [7] used in our work, and their histograms.

The three reference images in Figure 1 were used by an artist to sketch the image features which formed our base synthetic image (Figure 2). The histogram of the synthetic image bears similarity with those of the reference images.

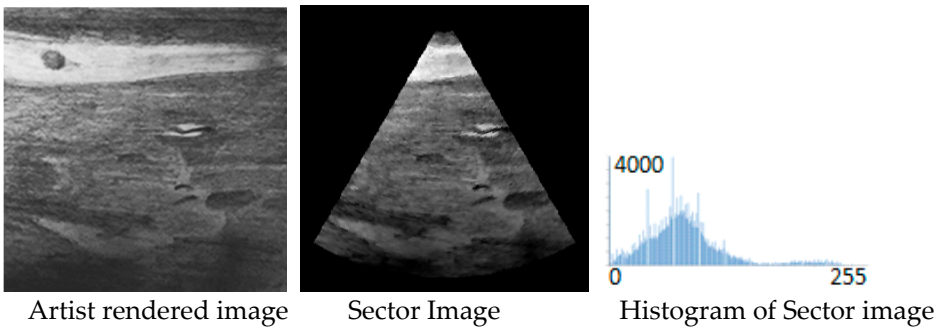

Figure 2. Artist rendered synthetic image, and Sector image and its histogram.

The main methods used in the speckle simulation modelling and evaluation pipeline are depicted in Figure 3. Within the simulation model, the synthetic image is first sampled based on an acquisition model, speckle noise is then generated at the sampled points, and an interpolation algorithm used to fill the sector scan region. The evaluation model uses image quality metrics computed for the output are then compared with those of the reference ultrasound images for a quantitative assessment of the quality of the final synthetic images. A subjective evaluation is also performed using expert sonographers. In consideration of subjective evaluation, texture feature analysis is performed using local binary patterns in order to validate subjective assessment and equate results to human perception of texture.

Preprints (www.preprints.org) | NOT PEER-REVIEWED | Posted: 30 October 2017 doi:10.20944/preprints201710.0181.v1

Peer-reviewed version available at J. Imaging 2018, 4, 3; doi:10.3390/jimaging4010003

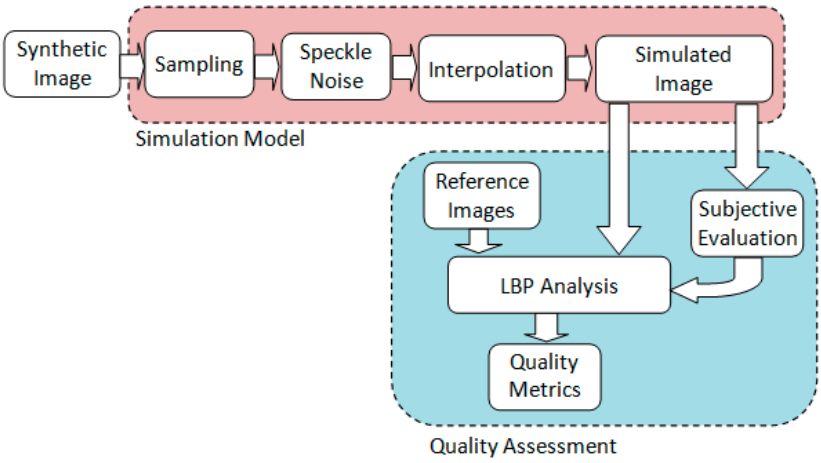

Figure 3. The simulation and evaluation stages of the processing pipeline.

The processing stages within the simulation model are further elaborated in the next section.

3. The Modeling and Speckle Simulation

The first stage of the sampling model is the method that generates a set of points at a coarse spatial resolution. The configuration of points models the loss of resolution of the ultrasound image due to pulse length, and also the scanning mode (sector or linear). One of the original contributions in this field is the paper by Perreault and Auclair-Fortier [9], where a radial-polar sampling model was introduced. We extend their work and propose three types of sampling methods called radial-polar, radial-uniform, and uniform grid. The first two are closely related to sector scan, while the third corresponds to a sampling in linear orthogonal directions (Figure 4).

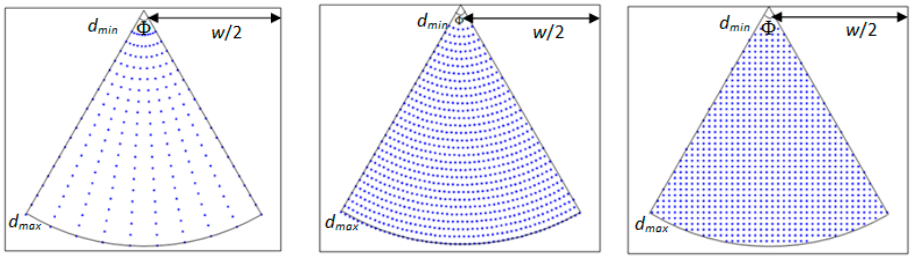

Figure 4. Sampling models that can be used in simulating speckle noise.

In Figure 4, the sector angle is denoted by Φ, and the extent of the sector is given by radial distances d_{min} and d_{max}. The image width is denoted by w. We also denote the total number of divisions along each radial line (axial resolution) by m, and the number of division of the sector angle (lateral resolution) by n. The Cartesian coordinates of the sampled points for radial-polar sampling are given by

$$d_j = d_{min} + j(d_{max}-d_{min})/(m-1); \qquad \theta_i = (3\pi-\Phi)/2 + i\Phi/(n-1)$$

$$x(i, j) = d_j \cos\theta_i + w/2; \qquad y(i, j) = -d_j \sin\theta_i; \qquad i = 0..(n-1); \qquad j = 0..(m-1) \tag{1}$$

Preprints (www.preprints.org) | NOT PEER-REVIEWED | Posted: 30 October 2017 doi:10.20944/preprints201710.0181.v1

Peer-reviewed version available at J. Imaging 2018, 4, 3; doi:10.3390/jimaging4010003

The non-uniform spacing of points in the radial-polar sampling method causes the density of points to increase towards the sector's apex. The radial-uniform sampling method uses a constant arc length Δ between points along each arc to generate a uniform spacing between points. The equations for this sampling model are same as in eq. (1) except that the polar angle θ will now depend on both i and j as shown below.

$$\theta_{ij} = (3\pi - \Phi)/2 + i\Delta/d_j \tag{2}$$

In the radial uniform sampling scheme, the parameter equivalent to the lateral resolution n is the number of sampling points n_u along an arc at distance d_i given by

$$n_u = \Phi\, d_j/\Delta \tag{3}$$

The uniform grid is the simplest sampling model corresponding to a rectangular arrangement of uniformly spaced points with a constant distance δ between points. If a sector scan region is required, the points outside the region are clipped using the line equations of the two bounding edges. Using eq.(3), if $f(x, y, \theta_{min}) > 0$ or $f(x, y, \theta_{max}) < 0$, the point (x, y) is outside the sector region.

$$\theta_{min} = (3\pi - \Phi)/2; \qquad \theta_{max} = (3\pi + \Phi)/2$$

$$f(x, y, \theta) = (x - w/2)\sin\theta + y\cos\theta \tag{4}$$

More details and implementation aspects of the above three models are given in [13]. For speckle simulation, we use the method given in [7]. Their model is based on a complex distribution of incoherent phasors (u, v) given by a two-dimensional Gaussian function g_σ. The complex amplitude of each pixel is initialized with the square-root of the sampled intensity value. The number of incoherent phasors $M(x, y)$ at each pixel (x, y) is set as the value of a random number under a uniform distribution within a pre-specified range $[a, b]$. The incoherent phasors are generated and added M times to both the real and imaginary components of the complex value at each pixel. The noisy intensity value is then given by the amplitude of the complex number.

After generating speckle noise at the sampled points, we use an interpolation method to fill the empty space left by the sampling step. In general, the interpolated value at a specified coordinate (x, y) of an image I is computed by grouping the sample values at neighboring pixels (l, m) using the following formula [14]:

$$I(x, y) = \sum_{l,m \in Z} \varphi(x - l, y - m)\, I(l, m) \tag{5}$$

where, $\varphi()$ denotes a two-dimensional interpolation/synthesis function that provides the weights of the linear combination of sampled intensity values. Commonly used interpolation methods are B-Spline and cubic Hermite [15, 16]. In [9], the authors used an interpolation scheme using the Lanczos-3 kernel [14], [17-20].

4. Synthetic Ultrasound Images

The framework detailed above provides several options and parametric variations in each stage of the pipeline. As seen in Section 3, the three sampling methods and three interpolation schemes themselves give nine possible combinations. Each sampling scheme has its own set of parameters

that can be varied over a wide range of values. The speckle noise generation algorithm also has a set of statistical parameters governing the noise distribution.

The first row of Figure 5 shows the variations when the axial resolution m is increased in radial-polar sampling, keeping the lateral resolution fixed at n = 40. The interpolation used was Lanczos-3 [18].

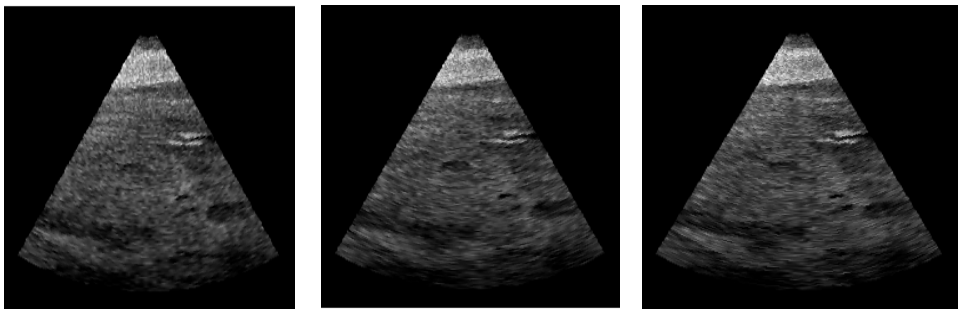

m = 120 m = 160 m = 200

Figure 5. Effect of changing axial resolution (m) in radial-polar sampling.

Similar results for radial uniform sampling are shown in Figure 6.

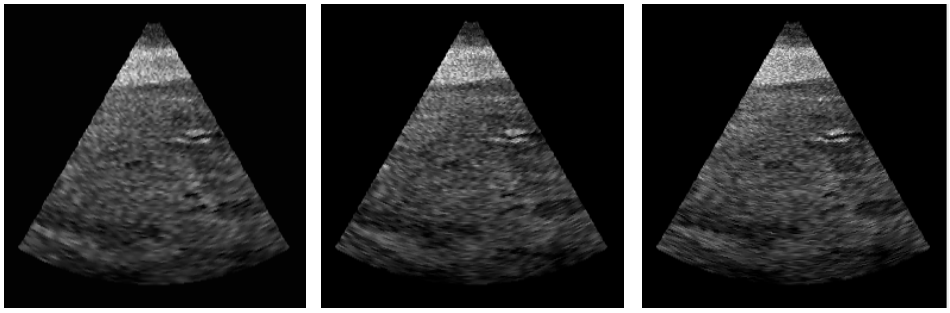

m = 120 m = 160 m = 200

Figure 6. Effect of changing axial resolution (m) in radial-uniform sampling.

Some of the commonly found artifacts in simulated images when values of certain parameters become large are shown in Figure 7. In Figure 7(a), a large value for m results in a dense, overlapping set of points along beam directions resulting in smoothing/merging of pixels. A similar effect is seen when both n and m are large (Figure 7(b)). When the σ value is large in the speckle generation function, the image becomes too grainy with loss of fine details, as in Figure 7(c).

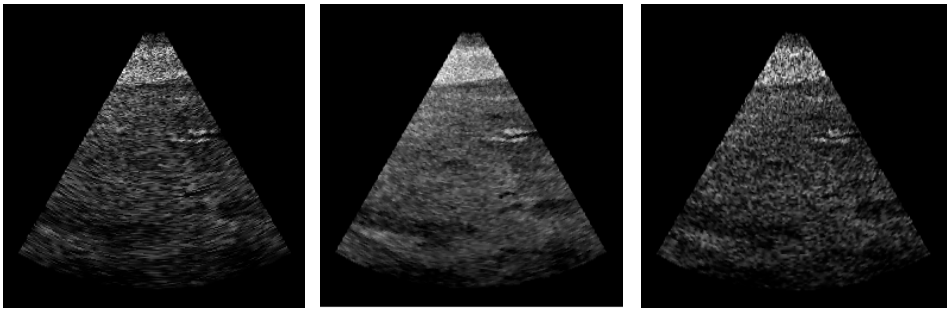

(a) n=40, m=240, σ=1.7 (b) n=60, m=160, σ=0.5 (c) n=80, m=120, σ=1.9

Figure 7. Image artifacts produced by large values of sampling and noise parameters

5. Analysis of Texture Features

One of the key requirements in the analysis of image modelling and simulation algorithms that use synthetic data is image quality assessment. Quality measures such as spatial frequency measure (SFM) and spectral activity measures (SAM) are commonly used in the assessment of image quality in the evaluation of compression and noise filtering algorithms [17]. In our prior work [21], we used entropy, SFM and SAM to compare the quality of the synthetic images with that of real ultrasound images. From that analysis, it became evident that we need to use higher order texture features to accurately characterize the desirable image properties, and to arrive at a robust set of quality metrics that conform to the subjective evaluations performed by expert clinicians. This paper presents a quality evaluation model using local binary patterns (LBP) and proposes a set of quality metrics (LBP feature values) that can provide consistent results on both synthetic and real ultrasound images. It has also been shown that synthetic images that give minimum feature deviation from real images are the ones that were given the highest subjective evaluation scores by experts, and therefore the proposed feature set contain sufficient information about the required texture features in the input synthetic images. In other words, these quality metrics determine the optimal set of sampling and noise parameters that would produce simulated ultrasound images closely matching the texture features of real ultrasound images. The images generated in this manner could be used to evaluate algorithms for speckle noise filtering (Figure 8).

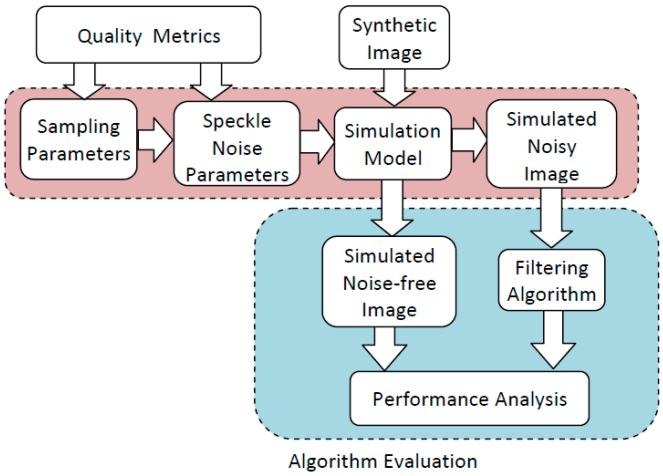

Figure 8. Application of the proposed LBP features in the evaluation of filtering algorithms.

5.1. Local Binay Patterns (LBP)

The irregularity and heterogeneity of texture features form the primary characteristics of ultrasound images and therefore play an important role in the assessment of their quality. A powerful texture descriptor that has been successfully applied in the field of medical image analysis is called the Local Binary Pattern (LBP) [22], [23]. This feature is derived by comparing the intensity at each pixel with its eight neighbors and encoding the information in an 8-bit integer value. This encoding can be viewed as a transformation of the input image into an LBP image as shown in Figure 9.

Preprints (www.preprints.org) | NOT PEER-REVIEWED | Posted: 30 October 2017 doi:10.20944/preprints201710.0181.v1

Peer-reviewed version available at J. Imaging 2018, 4, 3; doi:10.3390/jimaging4010003

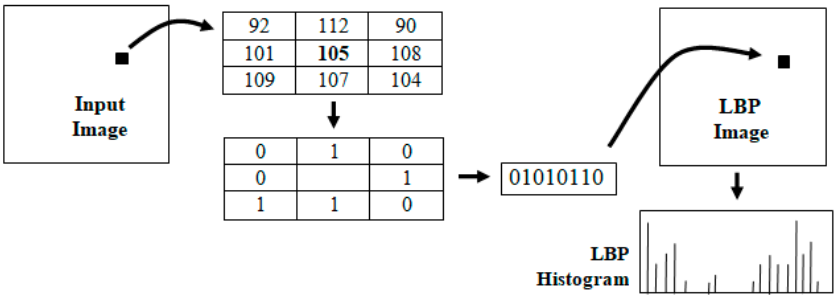

Figure 9. The intermediate steps in the computation of the LBP histogram of an image.

The histogram of the LBP image is generally used for texture classification [11]. In the area of medical image analysis, LBP methods have been successfully used in characterizing disease patterns [23]. There has also been a limited number of applications of local binary patterns in image quality assessment [10]. In this paper, we propose a novel approach for objective quality evaluation of synthetic ultrasound images using features derived from the LBP histogram.

5.2. LBP Features of Synthetic Ultrasound Images

The LBP histogram of ultrasound images contains predominant features that represent texture characteristics in the image. As an example, a synthetic ultrasound image of size 256x256 pixels, the corresponding LBP image and the LBP histogram are shown in Figure 10.

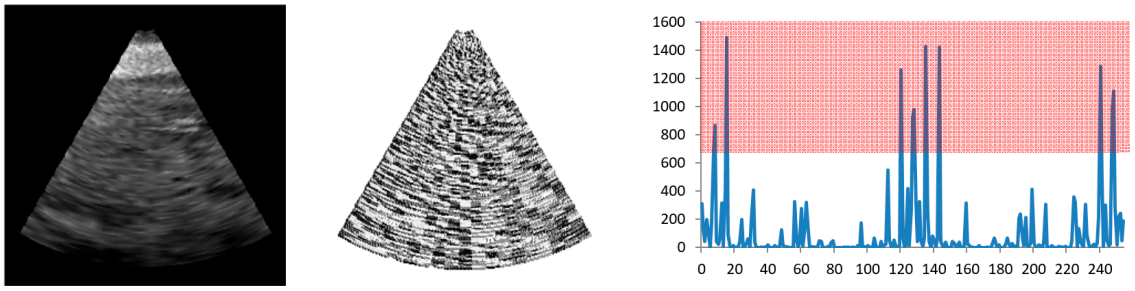

(a) (b) (c)

Figure 10. (**a**) A synthetic ultrasound image; (**b**) The LBP image; (**c**) the LBP histogram.

In Figure 10(c), we have highlighted the important LBP features based on their magnitudes. The LBP histogram contains 256 values L_i , i = 0…255. We propose the following feature vector consisting of eight LBP features for quality assessment:

$$V = \{L_8, L_{15}, L_{120}, L_{128}, L_{135}, L_{143}, L_{240}, L_{248}\} \quad (6)$$

The above features show consistent variations with changes in axial and lateral resolutions at the modelling stage. The next section discusses the experimental results in detail and also shows that the LBP features can also help select these modelling parameters so that the features closely match with those of real ultrasound images.

6. Experimental Analysis and Validation

6.1. LBP Feature Vector for Reference Images

The feature vector given in Equation (6) was computed for the three reference images in Figure 1, and the average of the three sets were used as the reference feature vector. These values are given below:

Preprints (www.preprints.org) | NOT PEER-REVIEWED | Posted: 30 October 2017 doi:10.20944/preprints201710.0181.v1

Peer-reviewed version available at J. Imaging 2018, 4, 3; doi:10.3390/jimaging4010003

$$V_{Ref} = \{447.3, 597.3, 508.7, 433.7, 691.7, 435.3, 459.3, 290\} \quad (7)$$

The reference values were used in our experimental analysis detailed in the following sections, to find the answers to three main research questions:

1. When the parameters controlling the resolution in a sampling method are adjusted from coarse to fine, do the values of the corresponding LBP feature vector consistently tend towards the reference feature vector?
2. Do the synthetic images that give feature values close to the reference vector also have consistently high subjective evaluation scores assigned by clinical experts?
3. Which one of the three modelling schemes generated feature values that are closest to the reference feature vector?

We performed an extensive analysis using LBP features by varying the sampling parameters for the radial polar, radial uniform and uniform grid methods, and the results are summarized below.

6.2. LBP Feature Vector for Radial-Polar Sampling

Here, we consider the images generated using the radial-polar sampling scheme. Quality analysis using global features such as entropy, SAM and SFM, and also subjective evaluations revealed that an axial resolution value (m in Equation 1) of 120, and speckle noise level $\sigma = 0.5$ gave acceptable results. We therefore fixed these parameters and varied only the lateral resolution (n in Equation 1) from 10 to 120. A few sample images are shown in Figure 11.

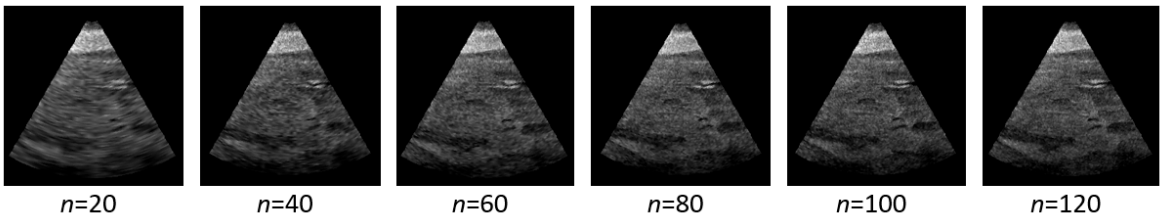

Figure 11. Synthetic images generated using radial polar sampling with a coarse to fine variation of lateral resolution parameter n.

The variations of each of the eight components of the feature vector (Equation 6) computed from the LBP histogram are shown in Figure 12.

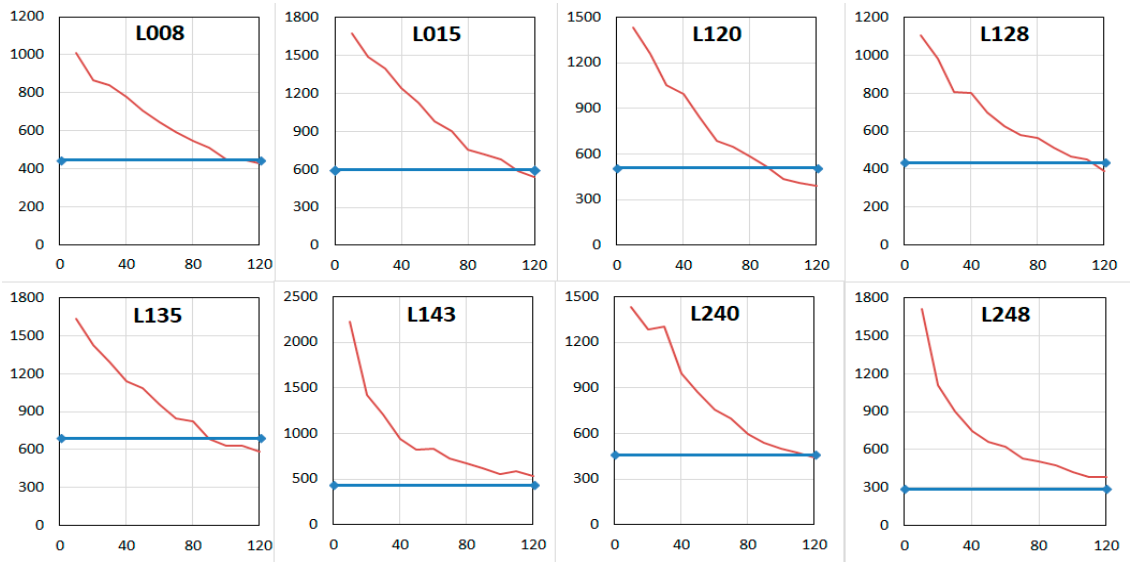

Peer-reviewed version available at J. Imaging 2018, 4, 3; doi:10.3390/jimaging4010003

Figure 12. Variations of LBP feature vector components with lateral resolution in radial-polar sampling. The x-axis gives the values of n.

In Figure 12, the blue horizontal lines indicate the values of the reference feature vector as given in Equation 7. All components of the LBP feature vector show consistent variations towards the reference values as the value of the lateral resolution parameter n is increased.

6.3. LBP Feature Vector for Radial-Uniform Sampling

The parameter affecting the lateral resolution in radial uniform sampling is n_u given in Equation 3. The effect of variation of this parameter in the quality of the synthetic images is shown in Figure 13.

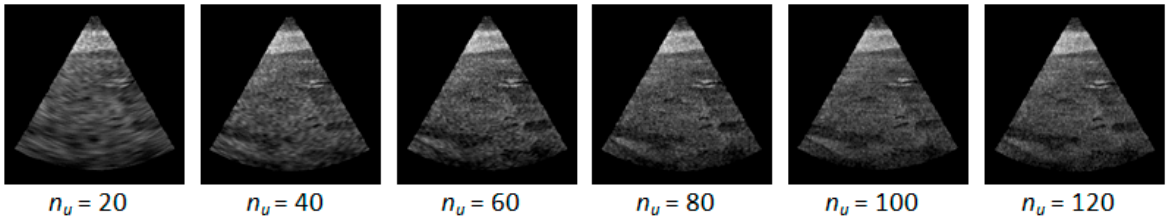

Figure 13. Synthetic images generated using radial uniform sampling with a coarse to fine variation of lateral resolution parameter n_u .

The variations of the LBP feature vectors (Equation 6) with n_u are shown in the graphs in Figure 14.

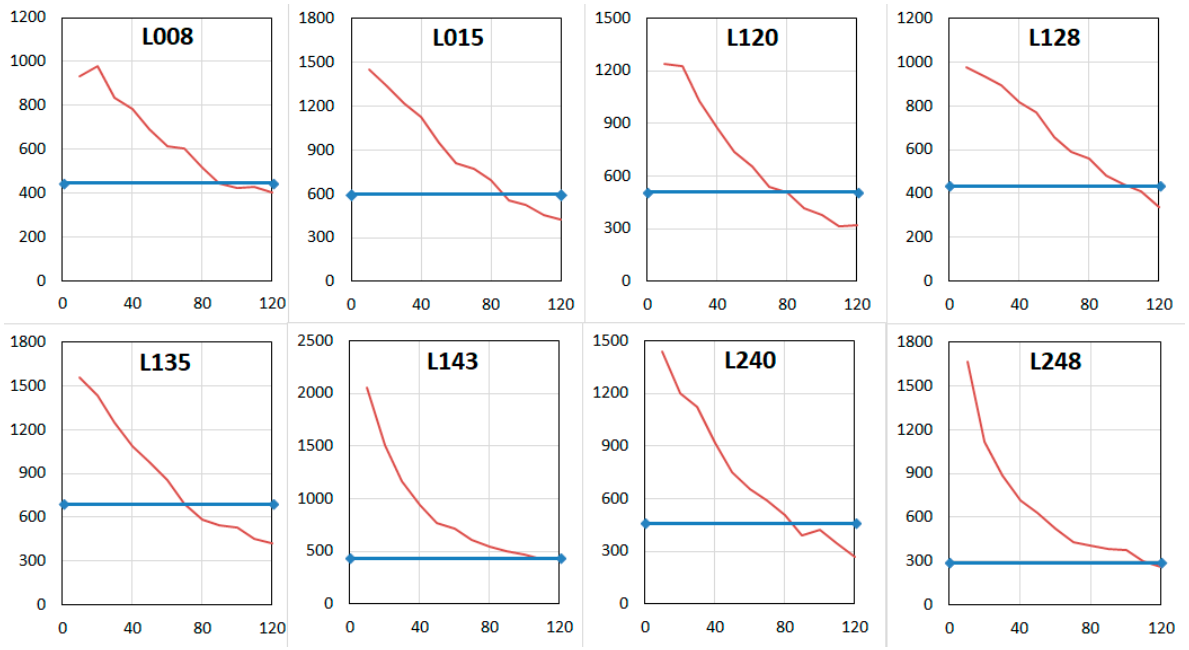

Figure 14. Variations of LBP feature vector components with lateral resolution in radial-uniform sampling. The x-axis gives the values of n_u.

In the case of radial uniform sampling also, we see a trend towards the reference values of the LBP features as the lateral resolution n_u of the images is increased from 10 to 120.

6.4. LBP Feature Vector for Uniform-Grid Sampling

As previously mentioned in Section 3, the uniform-grid sampling method uses a constant spacing δ between sampling points along both x and y directions. Therefore, increasing δ reduces the resolution of the sampled image in both directions. Consequently, we will get a fine to coarse variation of quality in the image as δ is increased, as shown in Figure 15.

Preprints (www.preprints.org) | NOT PEER-REVIEWED | Posted: 30 October 2017 doi:10.20944/preprints201710.0181.v1

Peer-reviewed version available at J. Imaging 2018, 4, 3; doi:10.3390/jimaging4010003

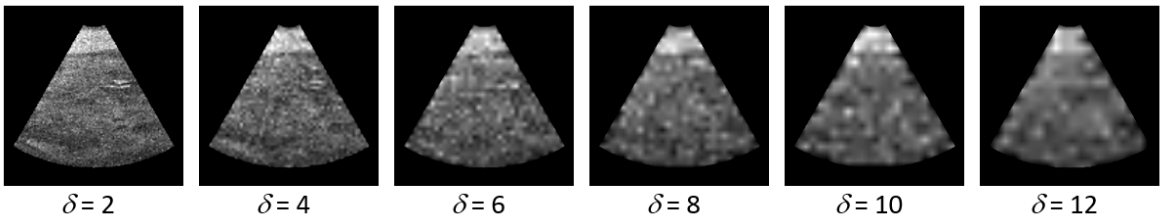

Figure 15. Synthetic images generated using uniform-grid sampling scheme with increasing values of the grid spacing parameter δ.

Since the image quality deteriorates as the value of δ is increased, the corresponding values of the LBP feature vector deviates further from the reference feature vector, as shown in Figure 16.

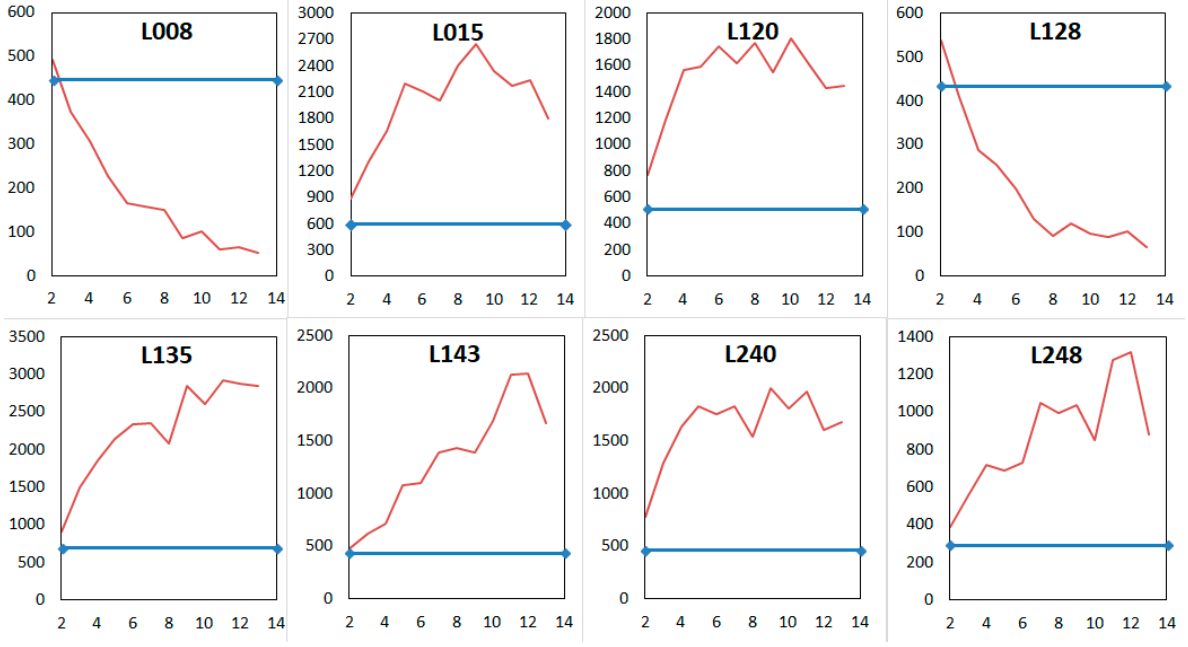

Figure 16. Variations of LBP feature vector components with grid spacing in uniform-grid sampling. The x-axis gives the values of δ.

6.5 Comparative Analysis of Sampling Techniques

The objective quality of the synthetic images produced by the three sampling methods is evaluated by computing the closest distance of the LBP feature vectors from the reference feature vector (indicated by the blue horizontal lines in Figures 12, 14, 16) using a Euclidean distance metric. The plots of the distance values for the three methods are given in Figure 17.

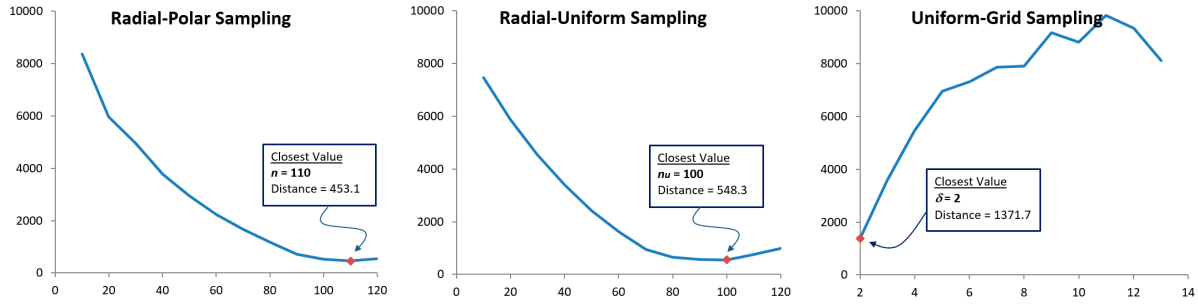

(a) (b) (c)

Figure 17. Plots showing the closest matching positions of the LBP feature vector with reference vector for images generated using (**a**) radial-polar sampling; (**b**) radial-uniform sampling; (**c**) uniform-grid sampling.

The comparative analysis showed that radial polar sampling with lateral resolution n = 110 gave the closest distance of the LBP feature vector from the reference feature vector. This result also matches very closely with the subjective evaluation scores reported in [21].

7. Conclusions and Future Work

This paper has presented the complete algorithmic framework for generating realistic and simulated ultrasound images incorporating image acquisition models, speckle noise formation processes and image interpolation schemes. The paper has introduced three sampling schemes, *viz.*, radial-polar, radial-uniform and uniform grid sampling methods. These methods together with the speckle simulation model and the interpolation scheme formed the simulation model of the processing pipeline. These processes within the simulation model allows users to vary a wide range of parameters that control the image and noise formation processes. The simulated images with speckle noise could be used to evaluate noise filtering methods as ground truth data (the corresponding synthetic images without noise) are readily available.

This paper has also presented detailed experimental study involving objective quality assessment using texture features derived from local binary patterns. The components of the LBP feature vector showed changes consistent with variations in the resolution of the synthetic images. More importantly, the values of the LBP features approached the values computed from real synthetic images, thus providing us an optimal set of modelling parameters that could be used for generating realistic synthetic images. The quality of such synthetic images was further validated using subjective evaluations performed by clinical experts.

Future work is directed towards using the proposed algorithm on a wider range of ultrasound images to analyse deviations in the values of LBP feature components and to evaluate the robustness of the selected LBP features under variations in imaged objects and tissue characteristics.

References

1. Zhang, J.; Cui, W.; Wu, L.; Lin, G.; Cheng, Y. A novel algorithm based on wavelet-trilateral filter for de-noising medical ultrasound images. *In: Control and Decision Conference* 2014, 3804-3809, DOI: 10.1109/CCDC.2016.7531648.
2. Malutan, R.; Terebes, R.; Germain, C.; Borda, M.; Cislariu, M. Speckle noise removal in ultrasound images using sparse code shrinkage. *In: IEEE international conference on E-health and bioengineering* 2015, 1-4, DOI: 10.1109/EHB.2015.7391394.
3. Le, T .Adaptive noise reduction in ultrasound imaging. *In: IEEE symposium on signal processing in medicine and biology* 2014, 1-1, DOI. 10.1109/SPMB.2014.7002961.
4. Zang, X.; Bascom, R.; Gilbert, C.; Toth, J.; Higgins, W. Methods for 2D and 3D endobronchial ultrasound image segmentation. *IEEE Trans. on Biomedical Engineering* 2016, *63(7)*, 1426-1439, DOI:10.1109/TBME.2015.2494838.
5. Cortes, C.; Kabongo, K.; Macia, I.; Ruiz, O.E.; Florez, J. Ultrasound image dataset for image analysis algorithms evaluation. In: Chen YW, Torro C, Tanaka S, Howlett R, Jain L. (eds) Innovation in Medicine and Healthcare. *Smart Innovation, Systems and Technologies* 2016, *45*, Springer, 447-457 DOI: 10.1007/978-3-319-23024-5_41.
6. Telmed Ultrasound Medical Systems. *http://www.pcultrasound.com/products/products_usimg/index.html*.
7. Ultrasound Image Gallery. *http://www.ultrasound-images.com/*.
8. Loizou, C.P.; Pattichis, C.S. *Despeckle Filtering for Ultrasound Imaging and Video*, Vol I.; Algorithms and Software. Morgan & Claypool, 2015; pp. 180; ISBN: 978-1-62705-668-7.
9. Perreault, C.; Auclair-Fortier, M.F. Speckle simulation based on B-mode echographic image acquisition model. *In: 4th Canadian conference on computer and robot vision* 2007, 379-386, DOI: 10.1109/CRV.2007.61.

10. Pietikainen, M.; Zhao, G.; Hadid, A.; Ahonen, T. *Computer Vision Using Local Binary Patterns,* Springer-Verlag, London, pp. EI-E2, ISBN: 978-0-85729-748-8.
11. Zhang, M.; Xie, J.; Zhou, X.; Fujita, H. No reference image quality assessment based on local binary pattern statistics. *Visual Communications and Image Processing (VCIP)* 2013, DOI:10.1109/VCIP.2013.6706418.
12. Singh, P.; Mukundan, R.; de Ryke R. Quality analysis of synthetic ultrasound images using second order statistical features. *In: Image and Vision Computing (IVCNZ2017*) 2017, paper accepted.
13. Singh, P.; Mukundan, R.; de Ryke R. Synthetic Models of Ultrasound Image Formation for Speckle Noise Simulation and Analysis. *IEEE International Conference on Signals and Systems* 2017, 278-284, DOI: 10.1109/ICSIGSYS.2017.7967056.
14. Somawirata, I.K.; Uchimura, K.; Koutaki, G. Image enlargement using adaptive manipulation interpolation kernel based on local image data. *In: IEEE International conference on signal processing, communication and computing* 2012, 474-478, DOI: 10.1109/ICSPCC.2012.6335692.
15. Kai-yu, L.; Wen-dong, W.; Kai-wen, Z.; Wen-bo, L.; Gui-li, X. The application of B-spline based interpolation in real-time image enlarging processing. *In: 2nd International conference on systems and informatics* 2014, 823-827, Doi: 10.1109/ICSAI.2014.7009398.
16. Goceri, E.; Lomenie, N. Interpolation approaches and spline based resampling for MR images. *In: 5th International symposium on health informatics and bioinformatics* 2010, 137-143, DOI: 10.1109/HIBIT.2010.5478891.
17. Xia, Z.W.; Li, Q.; Wang, Q. Quality metrics of simulated intensity images of coherent ladar. *In: International conference on optoelectronics and microelectronics* 2010, 214-216, DOI: 10.1109/ICoOM.2012.6316255.
18. Mirza, S.; Kumar, R.; Shakher, C. Study of various preprocessing schemes and wavelet filters for speckle noise reduction in digital speckle pattern interferometric fringes. *Optical Engineering* 2005, *44(4)*. DOI: 10.1117/1.1886749.
19. Grgic, S.; Grgic, M.; Mrak, M. Reliability of objective picture quality measures. *Jnl. of Elec. Engg* 2004, *55(1-2)* 3-10, DOI: 10.1.1.138.6936.
20. Burger, W.; Burge, M.J. *Digital image processing: An algorithmic introduction using java,* Springer, 2008, pp. 565, ISBN: 978-1-84628-968-2.
21. Singh, P.; Mukundan, R.; de Ryke R. Modelling, Speckle Simulation and Quality Evaluation of Synthetic Ultrasound Images. *Communications in computer and information science*-723 2017, Springer International Publishing, 74-85, DOI: 10.1007/978-3-319-60964-5_7.
22. Zhang, J.; Marszalek, M. Local features and kernels for classification of texture and object categories: A comparative study. *Intl. Jnl. of Computer Vision* 2007, *73*(2), 213-238, DOI: 10.1007/s11263-006-9794-4.
23. Sørensen, L.; Shaker, S.B.; Bruijne, M. de. Quantitative Analysis of Pulmonary Emphysema using Local Binary Patterns, *IEEE Transactions on Medical Imaging* 2010, 29(2), 559-569, DOI: 10.1109/TMI.2009.2038575.